Vibrational entropy of $L1_2$ Cu_3Au measured by inelastic neutron scattering

P. D. Bogdanoff and B. Fultz
Keck Laboratory of Engineering Materials, mail 138-78, California Institute of Technology, Pasadena, California 91125

S. Rosenkranz
Materials Science Division, Argonne National Laboratory, Argonne, Illinois 60439

(Received 28 January 1999)

The phonon density of states of elemental Au, Cu, and Cu_3Au with $L1_2$ chemical order were measured by inelastic neutron scattering and used to calculate the vibrational entropy of formation of the ordered compound from the elemental metals. A vibrational entropy of formation of $(0.06\pm0.03)\,k_B$/atom at 300 K was obtained, with the vibrational entropy of the ordered alloy being larger than that of the elemental metals. The phonon DOS of the disordered Cu_3Au was simulated by adding the phonon DOS curves of fcc Cu, $L1_2$ Cu_3Au, and fcc Au to match the numbers of first-nearest-neighbor pairs in a disordered alloy. The vibrational entropy obtained with this simulated DOS disagrees with calorimetric data and theoretical estimates, indicating that the phonon DOS of disordered Cu_3Au depends on chemical order at spatial lengths larger than is set by first-nearest-neighbor pairs. [S0163-1829(99)02429-7]

I. INTRODUCTION

The free energy and the phase diagram of Cu-Au alloys have long been topics of theoretical and experimental investigations. For example, the capabilities of the cluster variation method for obtaining configurational entropies were demonstrated by calculations on Au-Cu.[1–4] On the other hand, the influence of vibrational entropy on the thermodynamics of Au-Cu alloys has been largely ignored until recently. Earlier assessments of the lattice dynamics of ordered and disordered Cu_3Au have been conflicting and controversial[5–12] as discussed recently.[13]

The vibrational entropies of Cu-Au alloys are now receiving more attention. Cleri and Rosato (1993) calculated interatomic force constants with a tight-binding method. They used their force constants in a Born–von Kármán model to obtain $0.12\,k_B$/atom for the difference in entropy of the disordered and ordered alloys of Cu_3Au. Nagel, Anthony, and Fultz performed experimental measurements on the heat-capacity difference between ordered and disordered Cu_3Au, and obtained $(0.14\pm0.05)\,k_B$/atom when the low-temperature results were extrapolated to high temperatures in a harmonic approximation.[13] These results from calorimetry were compared to heat capacities calculated with phonon DOS curves deduced from previous measurements of phonon-dispersion curves of disordered and ordered Cu_3Au.[14,15] The difference in heat capacity obtained from the phonon DOS curves had the right sign, but exceeded the value obtained from the calorimetry data. This likely results from the unavoidable use of the virtual crystal approximation to interpret the coherent inelastic neutron scattering from the disordered alloy. Quite recently, Ozoliņš, Wolverton, and Zunger used a cluster expansion of results from first-principles calculations to obtain a difference in vibrational entropy of $0.06\,k_B$/atom at 300 K.[16] Their cluster expansion method is an approach which addresses the difficult problem of the phonon DOS of the disordered alloy.

A simpler problem is understanding the vibrational entropy of formation of the ordered $L1_2$ structure of Cu_3Au from elemental fcc Cu and fcc Au. The compound and the elemental constituents have true translational periodicity, so their phonon DOS curves are well defined. In their theoretical study, Ozoliņš, Wolverton, and Zunger obtained $0.1\,k_B$/atom for the vibrational entropy of formation at 800 K within the harmonic approximation, and $0.2\,k_B$/atom including anharmonic contributions.[16] Experimentally, using phonon DOS curves taken from the literature,[15,17,18] the vibrational entropy of formation is 0.07 k_B/atom, again with the compound having a higher vibrational entropy than the constituent elements. However, because the phonon measurements were performed by different investigators at different times, it is not clear whether the theoretical or experimental value is more reliable. We therefore made measurements under identical experimental conditions to obtain the phonon DOS of fcc Au, fcc Cu, $L1_2$ Cu_3Au, and a 3:1 mixture of elemental Cu and Au powders.

Within the harmonic approximation, we obtain a vibrational entropy of formation of $L1_2$ Cu_3Au from fcc Au plus fcc Cu in a 1:3 ratio of $(0.05\pm0.03)\,k_B$/atom at 250 K, and $(0.055\pm0.03)\,k_B$/atom at 800 K, with the ordered compound having the higher entropy. Using data on thermal expansion and bulk modulus, we obtain an anharmonic correction to the vibrational entropy of $(0.06\pm0.02)\,k_B$/atom at 800 K. In a second effort, the entropy of ordering of $L1_2$ Cu_3Au is estimated by combining the measured phonon DOS curves of the fcc Au, $L1_2$ Cu_3Au, and fcc Cu in proper proportions to match the first-nearest-neighbor pair correlations in the disordered alloy. The result of $-0.08\,k_B$/atom is in poor agreement with the result of $(0.14\pm0.05)\,k_B$/atom obtained previously by calorimetry. The phonon DOS of the disordered Cu_3Au alloy depends on chemical order at spatial lengths beyond that set by first-nearest-neighbor pairs.

II. EXPERIMENTAL

Four samples were prepared for neutron scattering, three in plate form and one as a powder. Au shot of 99.99% purity

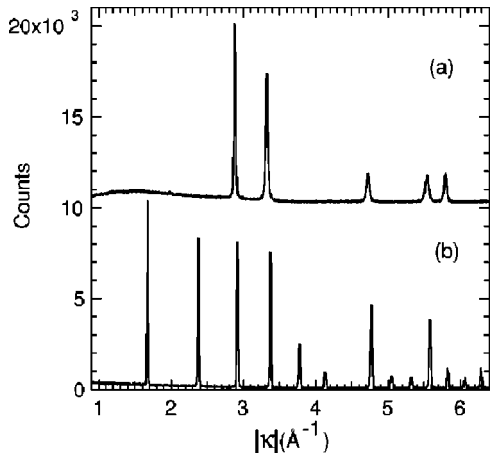

FIG. 1. X-ray-diffraction data for Cu_3Au plate. (a) before anneal, (b) after anneal.

was arc melted as a 66 g ingot. Filings of 25 g mass were prepared for use in the mixed powder sample, and the remainder was cold rolled to 0.029 cm thickness and used in sheet form as the sample of elemental Au. The elemental Au sheets were cut and assembled into a mosaic sample of uniform thickness of dimensions 7×9 cm and mass 36.61 g. The elemental Cu sample of 99.99% chemical purity was a plate of 7×9 cm with a thickness of 0.1 cm and mass 62.21 g.

The alloyed Cu_3Au sample was prepared by surface etching Cu shot of 99.999% purity, then arc melting the Cu with Au shot of 99.99% purity to form six button ingots of the correct composition. The ingots were cold rolled to 0.059 cm thickness. X-ray diffractometry with Co $K\alpha$ radiation using an Inel position sensitive detector was used to measure lattice parameter and chemical order. A representative diffraction pattern of as-rolled plate, presented in Fig. 1(a), shows a fcc material with no long-range order. Using the Nelson-Riley extrapolation method,[19] its mean lattice parameter was found to be 3.755 ± 0.002 Å. The rolled ingots were then sealed in evacuated pyrex and annealed at 650 K for 7 days, 635 K for 2 days, 623 K for 3 days and 608 K for 2 days. A representative diffraction pattern from these annealed plates is shown in Fig. 1(b). The data show a high degree of chemical ordering, which we determined to be 0.93 ± 0.05, with the uncertainty originating primarily from crystallographic texture. The mean lattice parameter of the annealed samples was 3.742 ± 0.001 Å. The annealed plates were cut and assembled into a mosaic plate of dimensions 7×9 cm and mass 43.7 g.

For the preparation of the powder sample, the Au filings were annealed at 1073 K for 1 h in an evacuated quartz ampoule and mixed with fine Cu powder (0.1 mm diameter) in a ratio of 3 Cu atoms per Au atom. The final weight of the powder sample was 36.67 g. All samples were encased in thin-walled Al pans for mounting in the displex refrigerator of the LRMECS spectrometer.

Inelastic neutron-scattering spectra were measured with the time-of-flight (TOF) chopper spectrometer LRMECS, at the IPNS spallation neutron source at Argonne National Laboratory. The plates and powder samples were mounted at a 45 deg angle normal to the incident beam in order to minimize self shielding. Scattering for the four samples; Cu, Au, $L1_2$ Cu_3Au, and mixed powders were 10%, 2%, 5%, and 4%, respectively. Spectra with an incident energy E_i of 35 meV were measured at 10 and 250 K for all samples and an empty container. A run with an absorbing cadmium sheet in the sample position was measured at room temperature to improve the background correction. Detector response was calibrated with a white beam vanadium run, and the instrumental resolution function was determined with a vanadium run taken with $E_i=35$ meV. The continuous detector coverage on LRMECS, ranging from 3 to 117 deg, allowed a simultaneous probe of the spectral response over a large range of momentum and energy transfer ($\boldsymbol{\kappa}$, $\hbar\omega$), with $|\boldsymbol{\kappa}(\omega)|$ varying between 0.2 and 7 Å^{-1} at zero energy transfer.

III. ANALYSIS AND RESULTS

A. Phonon density of states

All TOF spectra were first normalized and corrected for detector efficiency and time-independent background following standard procedures. In this step, the detectors were combined into groups spanning 10 deg each with average angles from 5 to 115 deg. The scattering contribution of the container and displex to the observed spectra was determined using the runs on the empty container and Cd sample, and taking into account the sample absorption. The data below 3–4 meV are dominated by the large elastic peak, which was stripped from the data with the following procedure. The data from 0 to 8 meV were modeled as the sum of a Gaussian function convolved with the instrument resolution function and the self-consistent 1–5-phonon contributions [from Eqs. (2)–(4)]. The modeled elastic peak was subtracted from the raw data, leaving the self-consistent phonon intensity below 3 meV. The phonon density of states was determined from the corrected spectra with the procedure outlined below.

1. Multiphonon corrections

The partial differential cross section for a harmonic Bravais lattice is given in the incoherent approximation as[20,21]

$$\left(\frac{\partial^2\sigma}{\partial\Omega\,\partial E}\right)^{\text{inc}}=\frac{\sigma_{\text{inc}}}{4\pi}\frac{k'}{k}\frac{N}{2\pi\hbar}e^{-2W}\int e^{\langle UV\rangle}e^{(-i\omega t)}dt, \quad (1)$$

where $U=-i\boldsymbol{\kappa}\cdot\boldsymbol{u}(0)$ and $V=i\boldsymbol{\kappa}\cdot\boldsymbol{u}(t)$. The variables $\boldsymbol{u}(t)$, σ_{inc}, k', k, N, W, and $E=\hbar\omega$ are, respectively, the atomic displacement from equilibrium at time t, incoherent scattering cross section, final and initial neutron wave-vector magnitudes, number of atoms in the crystal, Debye-Waller factor, and energy transfer. Although the one-phonon expansion of Eq. (1) is a good approximation for small momentum transfer, the higher-order multiphonon terms cannot be neglected at higher scattering vectors, where the incoherent approximation is more reliable. The TOF spectra were measured at constant scattering angle, not constant scattering vector. The scattering vector therefore varies with energy transfer, and this dependence is different for each angle bank. Evaluating Eq. (1) while retaining the dependence of $\boldsymbol{\kappa}$ on ω, the following expression is obtained for the incoherent inelastic n-phonon double-differential scattering cross section:

$$\left(\frac{\partial^2\sigma}{\partial\Omega\,\partial E}\right)^{\text{inc}}_{n\text{-phonon}} = \frac{\sigma_{\text{inc}}}{4\pi\hbar}\frac{k'}{k}\frac{N}{n!}e^{-2W}\left(\frac{3\hbar}{2m}\right)^n [P(\omega)]^{n\text{-convolution}}, \tag{2}$$

where m denotes the mass of the scatterer,

$$P(\omega) = \frac{\langle(\boldsymbol{\kappa}\cdot\boldsymbol{e}_s)^2\rangle_\omega}{\omega} g(\hbar\omega)\langle n_\omega + 1\rangle + \frac{\langle(\boldsymbol{\kappa}\cdot\boldsymbol{e}_s)^2\rangle_{-\omega}}{-\omega} g(-\hbar\omega)\langle n_{-\omega}\rangle, \tag{3}$$

and

$$\left(\frac{\partial^2\sigma}{\partial\Omega\,\partial E}\right)^{\text{inc}}_{\text{inelastic}} = \sum_{n=1}^{\infty}\left(\frac{\partial^2\sigma}{\partial\Omega\,\partial E}\right)^{\text{inc}}_{n\text{-phonon}}. \tag{4}$$

The index s specifies a single vibrational mode and the notation $\langle\ldots\rangle_\omega$ denotes an average over all vibrational modes with frequency ω. The variable $\boldsymbol{e}_s$ is the phonon polarization vector of mode s. The function g is, as usual, the normalized phonon DOS. The notation $[f]^{n\text{-convolution}}$ specifies the sequential convolution of n instances of the function f. For example, $[P(\omega)]^{1\text{-convolution}} \equiv P(\omega)$ and $[P(\omega)]^{2\text{-convolution}} = \int_{-\infty}^{\infty} P(x)P(\omega - x)dx$. The term $\langle(\boldsymbol{\kappa}\cdot\boldsymbol{e}_s)^2\rangle_\omega$ simplifies to $\frac{1}{3}\boldsymbol{\kappa}(\omega)^2$ for a crystal with cubic symmetry, which was the case for all our samples.

As is seen from Eq. (2), the phonon DOS is obtained easily from the one-phonon cross section. The latter was derived in an iterative process from the measured spectra by evaluating Eq. (2) for the 1–5-phonon contributions, fitting their sum [Eq. (4)] plus a resolution-broadened Gaussian to the corrected data and subtracting the resolution-broadened Gaussian and 2–5 multiphonon contributions from the spectrum. The remaining intensity was then corrected for the thermal factor, cross section over mass (if applicable), and Debye-Waller factors (see Sec. III A 2). Mean-square displacements (for use in the Debye-Waller factor) were taken initially from the literature,[17,18,15] but then calculated self-consistently. The sum of the corrected intensities from all 12 angle banks gives the phonon DOS. By summing over the angle banks we ensure that a large portion of reciprocal space is sampled at each phonon energy. The resulting phonon DOS was then used to re-evaluate Eq. (2) and the procedure was iterated until the DOS converged. The first iteration was calculated by assuming the multiphonon contribution to be a constant. Given the phonon DOS, all cross sections of Eq. (2) can be calculated. The 1–5-phonon contribution as calculated using Eq. (2) fitted remarkably well the TOF spectra of elemental Au and Cu, but less well the spectra of the $L1_2$ Cu_3Au and mixed powders. This is to be expected for a model which assumes a single mass and scattering factor for an average atom. Nevertheless, since the multiphonon contributions are essentially featureless and small, the above procedure yields a sufficiently accurate correction for multiphonon scattering.

2. Debye-Waller, cross section, and mass corrections

For interpreting the TOF spectra of the binary $L1_2$ Cu_3Au alloy, the Debye-Waller, cross section, and mass corrections, which are different for Cu and Au atoms, were taken into account using the partial DOS of each species. The partial DOS curves were calculated from a Born–von Kármán model derived from phonon-dispersion curve measurements on single crystals.[15] The partial phonon DOS $g_d(E)$ of atom d is given by

$$g_d(E) = \sum_{\boldsymbol{q},j} |\boldsymbol{e}^d_{\boldsymbol{q},j}|^2 \delta(\hbar\omega_{\boldsymbol{q},j} - E), \tag{5}$$

where $\boldsymbol{q}$ and j are the phonon wave vectors and polarization branch and together specify a single vibrational mode; $\boldsymbol{e}^d_{\boldsymbol{q},j}$ and $\omega_{\boldsymbol{q},j}$ are, respectively, the polarization vector for atom d and frequency of mode $\boldsymbol{q}$, j. The correction factor is

$$\frac{Mg(E)}{\sum_{d=1}^{4} g_d(E)e^{-2W_d}(\sigma_d/m_d)}, \tag{6}$$

where $2W_d$, σ_d and m_d are, respectively, the Debye-Waller factor, the total scattering cross-section and the mass of atom d in the unit cell. M is a normalization factor, equal to the integral of the denominator over all energies. Au and Cu have very similar total scattering cross sections, but since m_{Au} is 3 times that of m_{Cu}, the modes with significant Au displacements are de-emphasized by up to a factor of 3 in the experimental data. Equation (6) has a momentum transfer dependence within the Debye-Waller factors, so the correction factor differed slightly for TOF spectra at different scattering angles. Typical correction factors for $L1_2$ Cu_3Au vary from 0.9 to 1.7 over the energy range, with the larger weighting occurring below 15 meV owing to the large Au displacements in the low-energy modes.

All $g(E)$ are normalized to unity with $\Sigma_d g_d(E) = g(E)$, and $g(E)$ and $g_d(E)$ were convolved with the instrument resolution function before being used to evaluate Eq. (6). In the case of the mixed powder sample, the Born–von Kármán elemental DOS for Cu $[g_{\text{Cu}}(E)]$ and Au $[g_{\text{Au}}(E)]$, and the sum $0.75g_{\text{Cu}}(E) + 0.25g_{\text{Au}}(E)$ were used for $g_{\text{Cu}}(E)$, $g_{\text{Au}}(E)$, and $g(E)$ in Eq. (6).

The final phonon DOS curves are shown in Figs. (2) and (3) together with the Born–von Kármán calculations. The composite DOS in Fig. 4 (see discussion in Sec. IV C) was constructed by summing the Au, Cu, and $L1_2$ Cu_3Au DOS with, respectively, the weights 0.06, 0.19, and 0.75.

B. Vibrational entropy

In the quasiharmonic approximation, the vibrational entropy, $S_{\text{vib}}(T)$ is calculated from $g(E)$ as

$$S_{\text{vib}}(T) = -3k_B\int_0^\infty g(E)[(n_E+1)\ln(n_E+1) - n_E\ln(n_E)]dE, \tag{7}$$

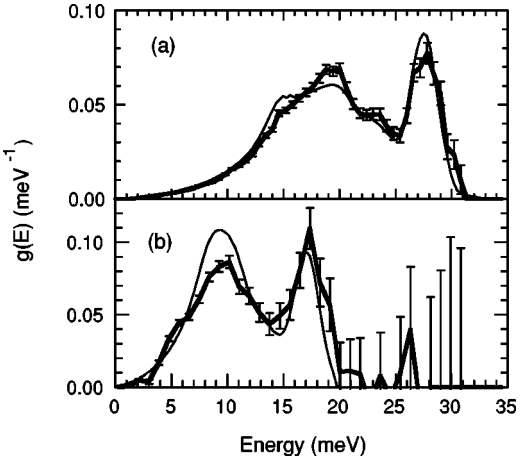

FIG. 2. Phonon DOS curves of (a) fcc Cu and (b) fcc Au. The thin lines are the result of a Born–von Kármán calculation (using force constants from Refs. 17, 18) convolved with an instrument resolution function. Cu and Au DOS curves have been normalized up to 32 and 20 meV, respectively.

where n_E is the Bose-Einstein distribution. To calculate the vibrational entropy of formation, $\Delta S_{\mathrm{vib}}^{\mathrm{form}}$, from the phonon DOS curves of the pure elements and the $L1_2$ Cu_3Au, we used the relationship

$$\Delta S_{\mathrm{vib}}^{\mathrm{form}}(T) = S_{\mathrm{vib}}^{\mathrm{Cu_3Au}}(T) - 0.75 S_{\mathrm{vib}}^{\mathrm{Cu}}(T) - 0.25 S_{\mathrm{vib}}^{\mathrm{Au}}(T), \quad (8)$$

and for the independent analysis using the mixed powders and the $L1_2$ Cu_3Au sample we used

$$\Delta S_{\mathrm{vib}}^{\mathrm{form}}(T) = S_{\mathrm{vib}}^{\mathrm{Cu_3Au}}(T) - S_{\mathrm{vib}}^{\mathrm{powders}}(T). \quad (9)$$

The anharmonic contribution to the vibrational entropy was calculated using the classical formula

$$S_{\mathrm{vib}}^{\mathrm{anh}}(T) = \int_0^T B v \beta^2 dT, \quad (10)$$

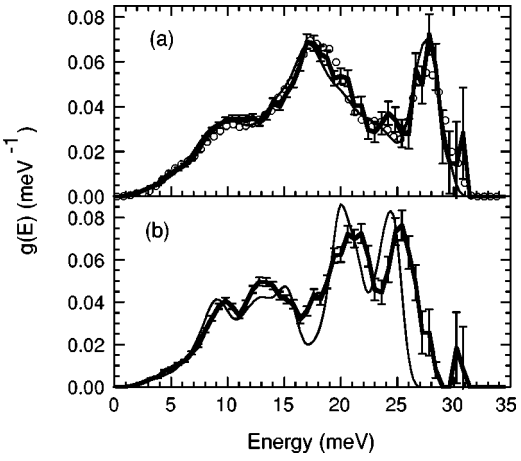

FIG. 3. Phonon DOS curves of (a) mixed Cu and Au powders and (b) $L1_2$ Cu_3Au. The thin lines are the result of Born–von Kármán calculations (using force constants from Refs. 15, 17, and 18) convolved with an instrument resolution function. The circles in (a) are a weighted sum of the thick curves in Fig. 2. The $L1_2$ Cu_3Au and powder DOS curves have been normalized up to 27 and 30 meV, respectively.

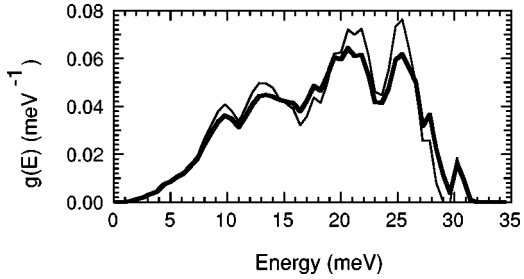

FIG. 4. The ''disordered'' thick curve is a composite phonon DOS curve comprising experimental phonon DOS curves in the fractions: 1/16 fcc Au, 3/4 $L1_2$ Cu_3Au, 3/16 fcc Cu, as described in part IV. The ''ordered'' thin curve is the $L1_2$ Cu_3Au curve of Fig. 3(b).

where B, v, and β are, respectively, the bulk modulus, the specific volume, and the coefficient of volume thermal expansion. Values for these variables were taken from the literature.[22–24] $S_{\mathrm{vib}}^{\mathrm{anh}}$ at 800 K was extrapolated from room temperature using Eq. (10) and B and β for $L1_2$ Cu_3Au, Cu, and Au. The uncertainty in the values for $\Delta S_{\mathrm{vib}}^{\mathrm{form}}$ at 800 K (see Table I) is a consequence of assuming that B and β are constant above room temperature. For Au, Cu, and $L1_2$ Cu_3Au we find that $S_{\mathrm{vib}}^{\mathrm{anh}}$ was 0.03, 0.05, and $0.05\,k_B$/atom at 300 K. The difference between the Cu_3Au and elemental metals was even smaller, being $0.005\,k_B$/atom at 300 K.

The values of $\Delta S_{\mathrm{vib}}^{\mathrm{form}}$ calculated from Eqs. (8)–(10) using the $g(E)$ shown in Figs. 2 and 3 are presented in Table I. Values labeled ''harmonic'' exclude the anharmonic contribution, and use Eq. (7) only, but the other values include the correction of Eq. (10).

IV. DISCUSSION

A. Phonon DOS curves

From Fig. 2 we observe that the phonon DOS curves from elemental Au and Cu agree well with the phonon DOS calculated with the Born–von Kármán model using force constants from single-crystal measurements.[15,17,18] The locations of the Van Hove singularities for the transverse and longitudinal modes agree reasonably well with the Born–von Kármán data, as do the energy cutoffs of the DOS. Our phonon DOS curves for both Au and Cu show an overall shift to slightly higher energies than the respective Born–von Kármán curves. We found only a small difference between the phonon DOS curves obtained at 10 and 250 K, so to improve statistics the data were summed.

In Fig. 3(b) the $L1_2$ Cu_3Au DOS is shown to be in reasonable agreement with the phonon DOS calculated with the Born–von Kármán model using force constants of Katano, *et al.*[15] The TOF data and the Born–von Kármán curves agree very well below 8 meV in the acoustic regime. At energies above 20 meV, the TOF results are shifted upwards by 1–2 meV with respect to the Born–von Kármán results. Anharmonic mode softening between our low-temperature data and room temperature could explain some, but not all, of this discrepancy.

TABLE I. Vibrational entropies of formation of $L1_2$-Cu_3Au.

	ΔS_{vib}^{form} (k_B/atom)			
T (K)	Mixed powders	Separate elements	Born–von Kármán[a,b]	Cluster expansion[c]
250 (harmonic)	0.05±0.03	0.05±0.03	NA	NA
300	0.06±0.03	0.05±0.03	0.07	NA
800 (harmonic)	0.06±0.03	0.05±0.03	NA	0.099
800	0.12±0.04	0.11±0.04	NA	0.201

[a]Reference 15.
[b]Reference 13.
[c]Reference 16.

B. Vibrational entropies of formation

Although all our phonon DOS curves were slightly stiffer than those calculated from the Born–von Kármán model using single-crystal data,[13,15] the differential values for ΔS_{vib}^{form} (listed in Table I) agree closely. Both experimental results are smaller than the results calculated by Ozoliņš, Wolverton, and Zunger,[16] but the difference is not much beyond experimental error.

By comparing Figs. 3(a) and 3(b), we see that the phonon DOS curves of the $L1_2$ Cu_3Au and the composite DOS of the elemental metals are similar at energies below 15 meV. The significant differences are the peak at 18 meV for the composite elemental DOS, the peak at 21 meV for $L1_2$ Cu_3Au, and the reduction of the peak from longitudinal modes in Cu at 28 meV to 26 meV for the optical modes in $L1_2$ Cu_3Au. Although the differences in peak positions are significant, the net change in the DOS curves upon formation of the compound is to move one peak up but another peak down. The net effect on ΔS_{vib}^{form} is therefore relatively small. We found good consistency between the phonon DOS curves measured on all samples at 10 and 250 K. Figure 3(a) also shows good consistency between the weighted sum of the phonon DOS curves of the elemental Cu and Au samples, and the composite DOS obtained from the mixed powders.

C. Disordered Cu_3Au

Although we have not measured the phonon DOS of the disordered alloy, it is possible to approximate it with the present results from fcc Au, $L1_2$ Cu_3Au, and fcc Cu. The idea is that the entropy can be expressed as a cluster expansion of the form

$$S_{vib} = S_0 + \sum_i S_i s_i + \sum_{ij} S_{ij} s_i s_j + \cdots , \qquad (11)$$

where the occupancy variables (or generalized spin variables) s_i and s_j are $+1$ when the site is occupied by a Cu atom, and -1 when occupied by an Au atom. The sum over pairs in Eq. (11) includes three constants S_{ij}, which correspond to the three pairs, Au-Au, Au-Cu, and Cu-Cu. The expansion of Eq. (11) is terminated at the first-nearest-neighbor (1NN) pair because only three phonon DOS curves are available. (It should be pointed out, however, that a model based on 1NN shells was successful for explaining the partial DOS of ^{57}Fe in ordered and disordered Fe_3Al.[25]) Half of the pairs in the ordered compound $L1_2$ Cu_3Au are Au-Cu pairs, the other half are Cu-Cu pairs. We can therefore solve for the appropriate mixture of phonon DOS curves required to simulate the disordered alloy by solving the following:

$$\begin{pmatrix} \text{Au-Au} \\ \text{Cu-Au} \\ \text{Cu-Cu} \end{pmatrix} = \begin{bmatrix} 1 & 0 & 0 \\ 0 & 1/2 & 0 \\ 0 & 1/2 & 1 \end{bmatrix} \begin{pmatrix} x_{\text{fcc Au}} \\ x_{L1_2\ \text{Cu}_3\text{Au}} \\ x_{\text{fcc Cu}} \end{pmatrix} . \qquad (12)$$

We obtain the fractions: $x_{\text{fcc Au}} = 1/16$, $x_{L1_2\ \text{Cu}_3\text{Au}} = 3/4$, $x_{\text{fcc Cu}} = 3/16$. The composite DOS curve obtained with these fractions and used in Eq. (7) is presented in Fig. 4, along with the phonon DOS curve of $L1_2$ Cu_3Au for comparison. From this phonon DOS curve of the disordered alloy we obtain a change in vibrational entropy of $-0.08\,k_B$/atom, meaning that the disordered alloy has a lower vibrational entropy than the ordered alloy. The sign of this result is in conflict with calorimetric data ($0.14 \pm 0.05\,k_B$/atom),[13] estimates by Ozoliņš, Wolverton, and Zunger ($0.06\,k_B$/atom),[16] and estimates using a virtual-crystal approximation for disordered Cu_3Au ($0.232\,k_B$/atom),[13] although this latter value is expected to be unreliable. The 1NN model of Eq. (11) is unsuccessful. Evidently the difference in vibrational entropy of ordered and disordered Cu_3Au depends on atomic correlations beyond 1NN pairs.

Perhaps the 1NN model is more successful when the structures used for the composite DOS have chemical compositions closer to that of the disordered alloy, as was the case for Fe_3Al.[25] To this end, we can use a different basis set of compounds and repeat the above analysis. Using fcc Cu and the ordered alloys $L1_2$ Cu_3Au and $L1_0$ CuAu a basis set, we obtain the fractions $x_{L1_0\ \text{CuAu}} = 3/8$, $x_{L1_2\ \text{Cu}_3\text{Au}} = 1/4$ and $x_{\text{fcc Cu}} = 3/8$ in the pair approximation to the disordered $L1_2$ Cu_3Au. Although a phonon DOS for $L1_0$ CuAu is not available, high-quality low-temperature heat-capacity measurements taken from the literature[26] were used to calculate $S_{vib}^{L1_0\ \text{CuAu}}$ and hence a vibrational entropy of disordering of $-0.01\,k_B$/atom. While this result is not accurate, it is an improvement over that from the basis set {Cu, $L1_2$ Cu_3Au, Au}.

Lastly, using all five ordered compounds and elements in the Au-Cu alloy system, we can go beyond the pair approximation. Matching the disordered Cu_3Au point, pair and tetrahedron correlations, we arrive at the following fractions: $x_{\text{fcc Cu}} = 0.3164$, $x_{L1_2\ \text{Cu}_3\text{Au}} = 0.4219$, $x_{L1_0\ \text{CuAu}} = 0.2109$, $x_{L1_2\ \text{CuAu}_3} = 0.0469$ and $x_{\text{fcc Au}} = 0.0039$. Although $S_{vib}^{L1_2\ \text{CuAu}_3}$ is completely unknown, its contribution is

weighted only at 5%. As a first approximation, we can assume that $S_{\mathrm{vib}}^{L1_2\ \mathrm{CuAu_3}} = 0.25 S_{\mathrm{vib}}^{\mathrm{fcc\ Cu}} + 0.75 S_{\mathrm{vib}}^{\mathrm{fcc\ Au}}$. We arrive at a value of $(-0.02 \pm 0.03)\, k_B$/atom for the vibrational entropy of disordering. While this is no better than our second result for the pair approximation, it was obtained with a wider range of alloy compositions. These three examples give hope that convergence to the correct vibrational entropy of the disordered alloy will occur with only modest sized clusters and a broad range of alloy compositions.

V. CONCLUSIONS

Time-of-flight inelastic neutron-scattering spectra were acquired with the LRMECS spectrometer on Cu_3Au with $L1_2$ chemical order, and from fcc Cu and fcc Au for comparison. A second comparison used a sample comprising mixed powders of Cu and Au in a 3:1 ratio. Data analysis was performed on energy spectra from 12 independent angle banks of detectors. The approach to the multiphonon and Debye-Waller corrections allowed for the variation of $|\kappa|$ with E in each of the 12 spectra. Phonon densities of states were obtained from the four samples, and were used to calculate the vibrational entropy of formation of the ordered compound from the elemental metals. Both comparisons gave a vibrational entropy of formation of $(0.06 \pm 0.03)\, k_B$/atom at 300 K, with the vibrational entropy of the ordered alloy being larger than that of the elemental metals.

The phonon DOS of the disordered Cu_3Au was approximated by making a composite phonon DOS from the phonon DOS curves of basis sets of compounds such as {fcc Cu, $L1_2$ Cu_3Au, fcc Au}. This involved matching the numbers of first nearest-neighbor pairs to those of a disordered alloy. This approach was generally unsuccessful, giving a vibrational entropy of ordering of the wrong sign or zero. Better choices of basis sets gave better results, however, suggesting that the phonon DOS of disordered Cu-Au alloys may be possible to obtain with clusters of modest size.

ACKNOWLEDGMENTS

This work was supported by the U.S. Department of Energy under Contract No. DE-FG03-96ER45572 and BES-MS, W-31-109-ENG-38.

[1] C. M. Van Baal, Physica (Utrecht) **64**, 571 (1973).
[2] D. de Fontaine, in *Solid State Physics: Advances in Research and Applications*, edited by H. Ehrenreich, F. Seitz, and D. Turnbull (Academic, New York, 1979), Vol. 34, p. 73.
[3] T. Mohri, Acta Metall. Mater. **38**, 2455 (1990).
[4] M. Asta, G. Ceder, and D. de Fontaine, Phys. Rev. Lett. **66**, 1798 (1991).
[5] D. B. Bowen, Acta Metall. **2**, 573 (1954).
[6] P. A. Flinn, G. M. McManus, and J. A. Rayne, J. Phys. Chem. Solids **15**, 189 (1960).
[7] A. G. Fox, Philos. Mag. B **50**, 477 (1984).
[8] C. G. Shirley and R. M. Fisher, Philos. Mag. A **39**, 91 (1979).
[9] B. Borie, Acta Crystallogr. **10**, 89 (1957).
[10] L. H. Schwartz and J. B. Cohen, J. Appl. Phys. **36**, 598 (1965).
[11] P. C. Gehlen and J. B. Cohen, J. Appl. Phys. **40**, 5193 (1969).
[12] P. Bardahn and J. B. Cohen, Acta Crystallogr., Sect. A: Cryst. Phys., Diffr., Theor. Gen. Crystallogr. **32**, 597 (1976).
[13] L. J. Nagel, L. Anthony, and B. Fultz, Philos. Mag. Lett. **72**, 421 (1995).
[14] E. D. Hallman, Can. J. Phys. **52**, 2235 (1974).
[15] S. Katano, M. Iizumi, and Y. Noda, J. Phys. F **18**, 2195 (1988).
[16] V. Ozoliņš, C. Wolverton, and Alex Zunger, Phys. Rev. B **58**, R5897 (1998).
[17] J. W. Lynn, H. G. Smith, and R. M. Nicklow, Phys. Rev. B **8**, 3493 (1973).
[18] E. C. Svensson, B. N. Brockhouse, and J. M. Rowe, Phys. Rev. **155**, 619 (1967).
[19] J. Nelson and D. Riley, Proc. Phys. Soc. London **57**, 160 (1945).
[20] G. L. Squires, *Introduction to the Theory of Thermal Neutron Scattering* (Dover, New York, 1978).
[21] S. W. Lovesey, *Theory of Neutron Scattering From Condensed Matter* (Clarendon, Oxford, 1984), Chap. 4.
[22] D. C. Wallace, *Thermodynamics of Crystals* (Dover, New York, 1972), App. 2.
[23] K. Tanaka and M. Koiwa, Intermetallics **4**, S29 (1996).
[24] Computer code TAPP 2.0, E. S. Microware, Hamilton, OH, 1991.
[25] B. Fultz, T. A. Stephens, W. Sturhahn, T. S. Toellner, and E. E. Alp, Phys. Rev. Lett. **80**, 3304 (1998).
[26] D. T. Hawkins and R. Hultgren, J. Chem. Thermodyn. **3**, 175 (1971).